ACS APPLIED MATERIALS & INTERFACES

Research Article

www.acsami.org

Assessing the Immunosafety of Engineered Nanoparticles with a Novel *in Vitro* Model Based on Human Primary Monocytes

Yang Li,[*,‡,○] Paola Italiani,[‡] Eudald Casals,[§] Dirk Valkenborg,[∥,⊥] Inge Mertens,[∥,⊥] Geert Baggerman,[∥,⊥] Inge Nelissen,[∥] Victor F. Puntes,[§,#,▽] and Diana Boraschi[‡]

[‡]Institute of Protein Biochemistry, National Research Council, 80131 Napoli, Italy

[§]Institut Català de Nanotecnologia, Campus of the UAB, 08193 Bellaterra, Spain

[∥]Flemish Institute for Technological Research, 2400 Mol, Belgium

[⊥]Center for Proteomics, University of Antwerp, 2020 Antwerp, Belgium

[#]Vall d'Hebron Institute of Research (VHIR), 08035 Barcelona, Spain

[▽]Institut Català de Recerca i Estudis Avançats, ICREA, 08010 Barcelona, Spain

Supporting Information

ABSTRACT: The possibility that nanomaterials could perturb the normal course of an inflammatory response is a key issue when assessing nanoimmunosafety. The alteration of the normal progress of an inflammatory response may have pathological consequences, since inflammation is a major defensive mechanism and its efficiency maintains the body's health. The immunosafety of engineered nanoparticles at nontoxic concentrations was investigated with the use of a human primary monocyte-based *in vitro* system, which reproduces in a simplified fashion the full course of the physiological inflammatory response, from initiation and development to resolution. The kinetics of expression and production of inflammatory and anti-inflammatory cytokines and the proteomic profiles were used for describing the inflammatory defensive response. We assessed the ability of gold and silver nanoparticles to trigger inflammation and to interfere with the course of an ongoing defensive reaction. While neither nanoparticle type was able to directly activate monocytes, silver nanoparticles could exacerbate the inflammatory response of monocytes but did not interfere with the resolution of the inflammatory reaction. These findings support the use of human primary monocyte-based *in vitro* assays for realistically investigating the effects of engineered nanoparticles on human innate immune responses, in order to predict the immunological risk of nanomaterials and implement safe nanoparticle-based applications.

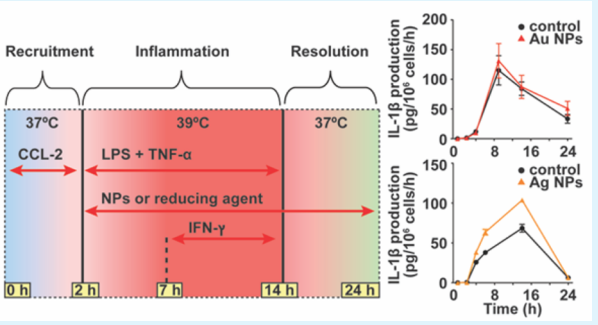

KEYWORDS: *nanoimmunosafety, human primary monocytes, in vitro model, proteomics, gold and silver nanoparticles*

1. INTRODUCTION

In the context of nanosafety, assessing the immunological safety of nanomaterials is an issue of major importance, given the key role of the immune system in avoiding invasion, defending the integrity of the body, and maintaining its health status.

Innate immunity is the first line of organisms' defense, providing an immediate reaction against infections and exogenous and endogenous insults. Evolutionarily conserved, innate immunity is active in all living organisms and is activated within minutes after encountering an infectious agent. In higher vertebrates, the more sophisticated adaptive immune response coexists with innate immunity and is activated at later times, only when the innate defenses are evaded or overwhelmed.[1] In the case of infection, the innate immune response activates a series of defensive mechanisms, such as phagocytosis, production of reactive oxygen species (ROS) and proteolytic enzymes, release of antimicrobial molecules, and production of inflammatory cytokines, which all contribute to developing the complex reaction that leads to killing and/or eliminating the infectious or foreign agents. The major cells involved in innate immunity are the phagocytic leukocytes, in particular macrophages, which are present in every tissue of the body with the role of patrolling and keeping the tissue "clean".[2] The innate defense reaction is activated in response to any "danger" signal (such as pathogens or foreign particles) and develops into a potent reaction aiming at eliminating the foreign agent. Once the danger is eliminated, in physiological healthy conditions the reaction is readily inactivated, to avoid excessive collateral damage to the surrounding tissues. A pathological condition occurs if the defensive responses are not properly down-

Received: May 25, 2016
Accepted: September 27, 2016

DOI: 10.1021/acsami.6b06278
ACS Appl. Mater. Interfaces XXXX, XXX, XXX−XXX

regulated and, for instance, persist for longer times, thereby causing tissue damage or facilitating deleterious autoimmune responses, as in the case of chronic inflammatory diseases.[2] In this context, a series of considerations should be made. First, we cannot consider "safe" nanoparticles that do not kill cells, because even if not directly toxic, they may interfere with the physiological cell functions.[3] Second, the immune system is constantly in action, getting activated and then silenced, in order to maintain the body integrity and functional homeostasis. Thus, "nontoxic" perturbations of the immune system caused by nanoparticles can become a health risk, if altering the complex network of immune reactions that ensure the body integrity. Lastly, we should bear in mind that the immune system is designed for dealing with microorganisms and foreign matter and nanoparticles belong to this category of agents. Based on the above considerations, it is clear that standard toxicity studies *in vitro* (such as membrane integrity, metabolic impairment, or DNA damage in cultured cells) or *in vivo* (*e.g.*, in severe combined immunodeficiency "SCID" mice) are not sufficient to determine the safe use of nanoparticles, as they do not consider the possibility that nontoxic nanoparticles may still have the capacity of perturbing cell functions. Therefore, immunosafety studies aiming at evaluating the effects of nanoparticles on innate immunity/inflammation should consider two scenarios. First, assessing the putative direct activation/inflammatory effect of nanoparticles: do nanoparticles directly trigger an innate/inflammatory reaction? Second, evaluating the possible interference (suppression or enhancement) by nanoparticles with the development of an innate reaction: do nanoparticles interfere with the normal development of a defensive response, either inhibiting it (causing immunosuppression) or enhancing it (provoking persistent/chronic inflammation)?[4] In order to address these issues, we have developed a novel human monocytes-based *in vitro* model, which accurately represents the human physiological inflammatory response.[5] In this study, we have applied this model to assessing nanoparticle interference with innate responses, in parallel with typical assays of *in vitro* activation of human primary blood leukocytes, using two metal nanoparticles (NPs), gold (Au) and silver (Ag), as prototypical examples.

Au NPs have many unique physicochemical and optical properties that could make them useful for biomedicine applications.[6−12] Studies on the safety of Au NPs for human use have addressed uptake and biodistribution,[13−15] cytotoxicity and biocompatibility,[16,17] and interaction with biological components.[18] Although many reports have shown that Au NPs are safe and nontoxic, other studies reported contrasting results.[19] On the other hand, Ag NPs have been extensively applied as antibacterial agents in many fields, such as health industry and textile coatings.[20−22] Despite decades of use and many reports regarding their cytotoxicity, genotoxicity, and biocompatibility,[23,24] the issue of Ag NP toxicity is still a matter of debate, with claims that toxicity depends on the released ions,[25−27] the NP evolution during storage and aging,[28] or the presence of biologically active contaminants.[29] The debate on the true potential of NPs for drug delivery was revamped by a recent study claiming that the past 10 years of research have brought to an efficiency of NP targeting to tumors of <1% of the administered dose, while the rest is either excreted through the renal clearance pathway or taken up by the mononuclear phagocyte system (MPS) in the various tissues and organs.[30] This observation underlines the importance of examining more in depth the interaction of NPs with phagocytic leukocytes, an interaction that is important both from the point of view of safety and from that of nanomedical effects.

In this study, we have synthesized sodium citrate-coated endotoxin-free 10 nm Au and 14 nm Ag NPs and used them *in vitro* for assessing their direct capacity of activating human blood leukocytes (in the whole blood assay and in the monocyte activation test). We also assessed their ability to interfere with an ongoing innate defensive response, using a kinetic monocyte-based *in vitro* model representative of a physiological resolving defensive reaction.

2. RESULTS

2.1. Characteristics of Nanoparticles. The characteristics of the Au and Ag NPs used in this study are reported in Figure 1 and Table 1. The Au NPs had a mean diameter of 10 nm,

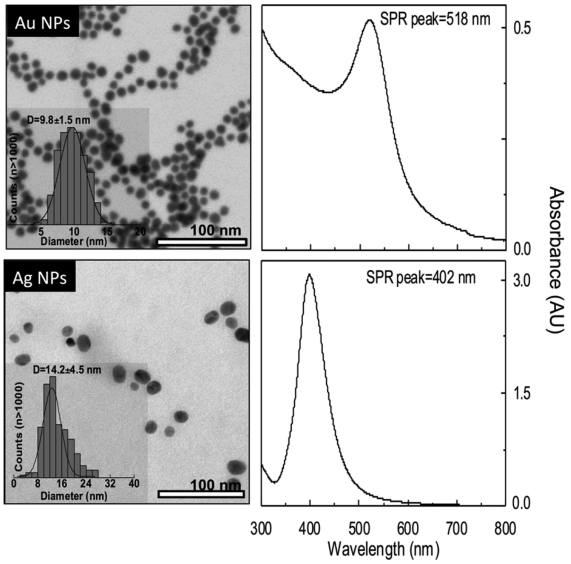

Figure 1. Characteristics of Au and Ag nanoparticles. Left panels: TEM images and size distribution profiles of Au (upper) and Ag NPs (lower). Right panels: UV−vis spectra of Au and Ag NPs.

while the Ag NPs were 14 nm in diameter, and both had a negative surface charge. The contamination with endotoxin (lipopolysaccharide, LPS) was assessed by the limulus amebocyte lysate (LAL) assay and found to be 0.45 EU/mL for Au NPs (32 μg/mL) and <0.17 EU/mL for Ag NPs (108 μg/mL) stock solutions (1 EU of endotoxin roughly corresponds to 100 pg), which are levels that allow one to work below the activation threshold (*vide infra*). After exposure in cell culture medium, both Au and Ag NPs can readily adsorb proteins from the medium forming a protein corona as previously reported.[31−33]

2.2. No Innate Immunity Activation by Au and Ag Nanoparticles *in Vitro*. In preliminary experiments, we have confirmed that the Au and Ag NPs used in this study do not induce death of human monocytes in cell culture at the selected endotoxin-free concentrations (<0.1−0.2 EU/mL; data not shown).[29] We thus tested the capacity of the two metal NPs to directly induce activation of innate immunity/inflammation, using two well-established and representative *in vitro* assays based on human primary blood cells. We used the whole blood assay (WBA) and the human monocyte activation test (MAT) for assessing the inflammatory potential of NPs, taking the production of the inflammatory cytokines at 24 h as activation

DOI: 10.1021/acsami.6b06278
ACS Appl. Mater. Interfaces XXXX, XXX, XXX−XXX

Table 1. Characteristics of the Nanoparticles Used in This Study

			stock concentration						
NP	size (nm)	pH	μg/mL	NPs/mL	cm^2/mL	nM	ζ-potential (mV)	reducing agent	LPS content (EU/mL)
Au	10	7	32	3.00×10^{12}	9.42	5.0	−45	2.2 mM sodium citrate	0.45
Ag	14	7	108	5.84×10^{12}	4.13	9.8	−50	10.0 mM sodium citrate	<0.17

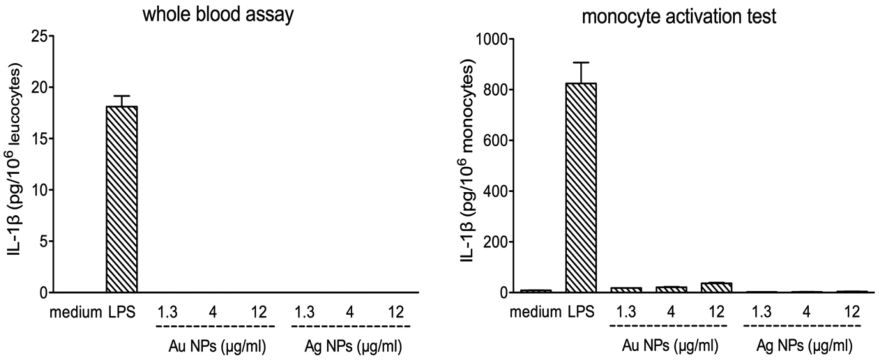

Figure 2. Effects of Au and Ag nanoparticles in whole blood assay and monocyte activation test. Au and Ag nanoparticles do not induce inflammation in the whole blood assay and monocyte activation test *in vitro*. Human whole blood (left) or human primary monocytes (right) were exposed to culture medium alone (negative control) or containing 1 ng/mL LPS (positive control) or increasing concentrations of Au or Ag NPs for 24 h. The production of IL-1β was measured by ELISA in the blood homogenates (WBA) or in the culture supernatants (MAT). Data are the mean ± SD of duplicates from one representative experiment (WBA) or of monocytes from three individual donors (MAT).

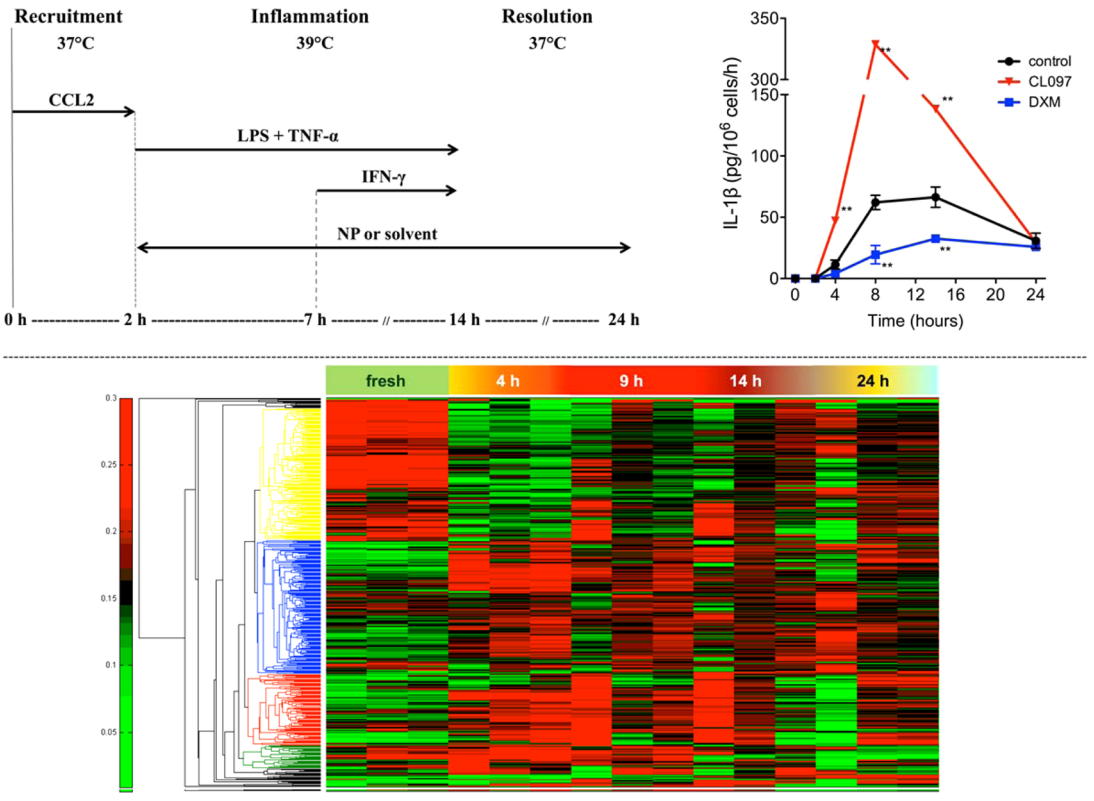

Figure 3. Human monocyte-based *in vitro* kinetic model of inflammation. Upper left panel: Schematic representation depicting the sequential steps of exposure of monocytes to inflammation-related stimuli to reproduce the inflammatory reaction and its resolution and to assess the possible effects of NPs on the reaction. Human primary monocytes were sequentially exposed in culture to CCL2 (20 ng/mL) from 0 to 2 h at 37 °C, to LPS (5 ng/mL) and TNF-α (10 ng/mL) from 2 to 14 h at 39 °C, to IFN-γ (25 ng/mL) from 7 to 14 h at 39 °C, and to medium alone from 14 to 24 h at 37 °C. NPs/solvent or other stimuli were present between 2 and 24 h. Upper right panel: Effect of the immunostimulatory agent CL097 (100 ng/mL) and of the anti-inflammatory drug DXM (10 μM) on the rate of IL-1β production during the course of the inflammatory reaction *in vitro*. Data are presented as the mean ± SD of replicate values within one representative experiment or from three to five replicate experiments. (*) $p < 0.05$; (**) $p < 0.01$ (vs control). Lower panel: Dendrogram of a hierarchical clustering analysis of the tandem mass tag (TMT) peptide intensities, which show different clusters of peptides varied during the inflammatory phase in this *in vitro* model. The proteomics heat-map represents the levels of expression of 489 nonredundant peptides, tested in monocytes from three individual donors at different time points.

DOI: 10.1021/acsami.6b06278
ACS Appl. Mater. Interfaces XXXX, XXX, XXX−XXX

end points. NPs were diluted in medium to concentrations that contained less than 0.2 EU of endotoxin/mL, taking this as an arbitrary threshold for lack of human monocyte activation (based on extensive in-house experience). Data in Figure 2 show that neither Au NPs nor Ag NPs could induce an appreciable production of IL-1β by human blood cells (either the whole leucocyte population or isolated monocytes). IL-1β was chosen as a reporter of the inflammation process, given its central role both in the inflammatory defense mechanisms and in inflammation-related diseases.[34] Similar results were obtained when assessing the production/expression of other inflammation-related cytokines, such as IL-6, IL-1α, IL-1β, and IL-36γ (see examples in Supporting Information Figures S1 and S2).

It is important to underline the fact that human innate immune cells are highly sensitive to endotoxin and strongly react to it. Thus, the absence of endotoxin contamination at the NP concentrations used in this study warrants that the possible activating effects are not due to the contaminating bioactive agents. To prove this fact, data in Figure S3 show that intentional contamination of Au NPs with endotoxin could turn them into highly inflammatory agents in the same assays (the example refers to IL-1β production in the MAT assay).

2.3. Model of Resolving Inflammation Based on Human Primary Monocytes. We have developed a kinetic *in vitro* model based on human primary monocytes that reproduces the course of the defensive inflammatory response (Figure 3, left panel). This model derives from a model we previously developed to represent the course of the inflammatory reaction brought about by inflammatory monocytes entering an inflamed tissue site.[5] Primary CD14$^+$ human blood monocytes were stimulated in culture with a sequence of stimuli and temperature changes (CCL2, LPS, TNFα, IFN-γ; 37 °C vs 39 °C), in order to reproduce the microenvironmental variations that occur during the development of an inflammatory reaction, from its onset until resolution. As shown in Figure 3, freshly isolated monocytes were exposed to the chemokine CCL2 for 2 h at 37 °C, to represent the CCL2 driven efflux of inflammatory monocytes from circulation to the site of inflammation. At 2 h, monocytes were exposed to the TLR4 agonist LPS, to mimic the encounter of inflammatory monocytes with infectious agents at the tissue site of reaction, and the temperature was raised to 39 °C. The development of the inflammatory reaction was reproduced by keeping the temperature at 39 °C from 2 to 14 h and by adding sequentially TNF-α at 2 h (representing the tissue/resident cell reaction) and IFN-γ at 7 h (representing the reaction of the later influx of Th1 cells). To reproduce the resolution of the inflammatory response, at 14 h all the inflammatory stimuli were washed off, the temperature was brought down to 37 °C, and fresh medium was added.

We have validated the inflammation model for its suitability to evaluating the modulating effects of exogenous agents. Data in Figure 3 (upper right panel) show that an immunostimulating agent (the synthetic TLR7/8 agonist CL097) and an immunosuppressive agent (the corticosteroid dexamethasone, DXM) added to monocytes during the development of the inflammatory response *in vitro* can significantly increase and decrease, respectively, the production of the inflammatory cytokine IL-1β. Accordingly, the same agents were effective in increasing and decreasing inflammatory activation of monocytes also in other conditions (Figure S4). This confirms that the monocyte responses in the kinetic model can be modulated, thereby confirming the suitability of the model for assessing immunomodulation by exogenous agents.

The transcriptomic profiling of the kinetic model was previously published[5] and showed that, among several inflammation-related factors, some genes of the IL-1 family, such as *IL1A* and *IL1B*, and *IL1RN* (coding for the cytokines IL-1α, IL-1β, and IL-1Ra) are differently regulated in the various phases of the inflammatory reaction. Being key effectors of inflammation and expressed exclusively during the inflammatory phase in our model, these cytokines represent relevant markers to investigate the inflammatory effects of NPs.

For further characterizing the *in vitro* model of inflammation, we analyzed the inflammation-related post-transcriptional variations. For a time-resolved (0, 4, 9, 14, and 24 h) description of the monocyte-based inflammation model at the protein level, a comprehensive proteomic analysis was performed to identify significantly altered expression patterns compared to fresh monocytes. The heat-map shown in Figure 3 (lower panel) represents 489 nonredundant peptides that varied at the different stages of the *in vitro* inflammation model, indicating that monocytes displayed a different proteomic profile during the inflammatory process *in vitro* compared to fresh monocytes.

In the dendrogram, four groups with differential expression patterns can be discerned (colored in yellow, blue, red, and green). Three peptide clusters (yellow, blue, and red) where sufficiently large to conduct a gene ontology enrichment analysis. For this purpose, we used the functional annotation charts of the DAVID web tool based on cellular component ontology and visualized the results in ReViGO tree-maps using the default settings. The tree-maps adapted from ReViGO are shown in Figure S5 for the biological process, molecular function, and cellular component ontologies, relative to the yellow, blue, and red clusters, respectively.[35] From these results, the blue cluster encompasses proteins that control the immune system development, programmed cell death, hydrogen peroxide metabolism, and homeostatic processes and shows low protein expression in fresh monocytes, up-regulation during inflammation, decrease during late inflammation, and resolution of the inflammatory reaction *in vitro* (Figure 3, lower panel). These results support the notion that this *in vitro* model can be used to represent the reactivity of inflammatory monocytes during the course of an inflammatory response. A more detailed analysis on these peptides is still ongoing.

2.4. Modulation of the Course of an Innate/Inflammatory Reaction *in Vitro* by Non-inflammatory Nanoparticles. To study possible perturbations of the *in vitro* inflammatory process, NPs were added to the monocyte cultures at the beginning of the inflammation phase (2 h) and left in until the end of the resolution phase (24 h). Figure 4 shows the profiles of gene expression and protein production for IL-1β and IL-1Ra upon exposure to Au NPs. These two cytokines were selected, among the several inflammation-related factors that are varied during the inflammatory response, because of their relevance in the development (IL-1β) and regulation (IL-1Ra) of inflammation.[34] Neither Au NPs (1.3 μg/mL) nor the Au NP solvent (2.2 mM sodium citrate solution) had any significant effect on the gene expression levels and on the protein production rates of the two cytokines throughout the entire course of the innate/inflammatory reaction. Likewise, Au NPs had no effect on the amount and kinetics of expression/production of other inflammation-related factors/cytokines, including IL-1α, IL-18,

DOI: 10.1021/acsami.6b06278
ACS Appl. Mater. Interfaces XXXX, XXX, XXX−XXX

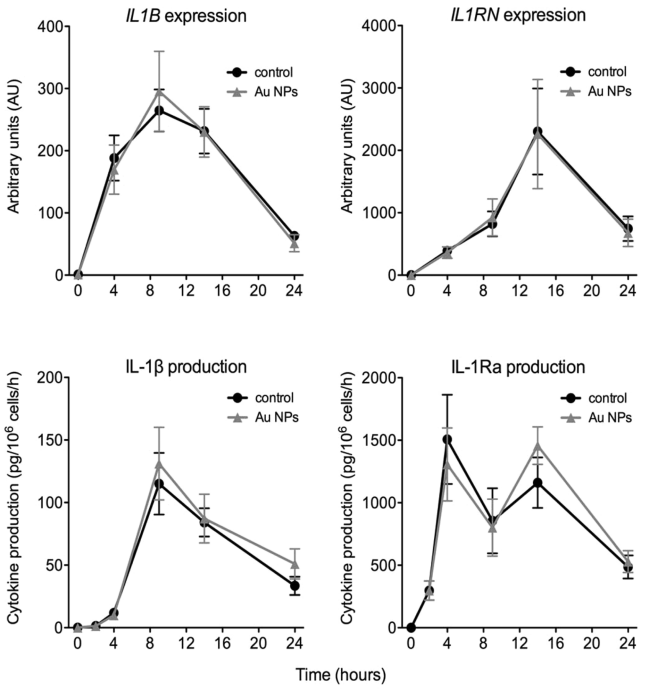

Figure 4. Effects of Au nanoparticles on the IL-1β and IL-1Ra gene expression and protein production during the course of the inflammatory reaction *in vitro*. Human primary monocytes were sequentially exposed to a series of stimuli and conditions that mimic the course of an inflammatory reaction, as shown in the Figure 3 left panel. Cultures were left untreated (solid dots) or exposed to 1.3 μg/mL Au NPs (triangles) from 2 to 24 h. Upper panels: Expression of *IL1B* and *IL1RN* genes (the genes encoding IL-1β and IL-1Ra, respectively). Lower panels: Rate of production/release of the cytokines IL-1β and IL-1Ra. Data are presented as mean ± SD of values obtained with monocytes from six to nine individual donors. Au NPs vs control: n.s. (not significant).

IL-36γ, IL-1R1, IL-1R2, IL-18BP, IL-6, and CCL5 (Table 2, and data not shown).

The lack of effects by Au NPs was confirmed in dose–response experiments showing that by increasing the NP concentration up to 12 μg/mL, no effect on either IL-1β or IL-1Ra could be observed (Figure S6). Note that these are standard concentrations in *in vitro* nanosafety studies.[36] We have also done a proteomics analysis of monocytes kinetically exposed to Au NPs, and preliminary data confirm that these NPs do not interfere with the ongoing inflammatory reaction (data now shown).

On the other hand, the presence of Ag NPs caused some variation in the course of the *in vitro* inflammatory reaction. At a concentration of 1.3 μg/mL, Ag NPs caused a small but significant increase in the production of IL-1β and a decrease in the production of its antagonist IL-1Ra during the full inflammation phases (4–14 h) (Figure 5, lower panels). The

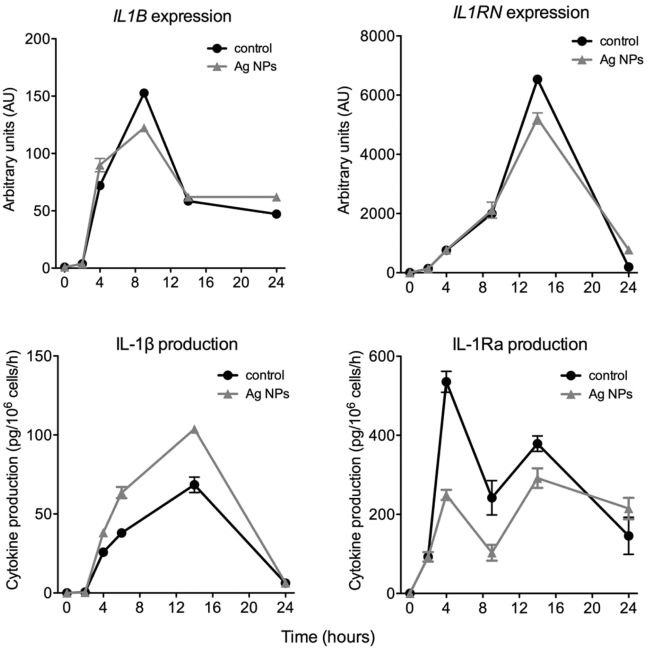

Figure 5. Effects of Ag nanoparticles on the IL-1β and IL-1Ra gene expression and protein production during the course of the inflammatory reaction *in vitro*. Human primary monocytes were sequentially exposed to a series of stimuli and conditions that mimic the course of an inflammatory reaction, as shown in the Figure 3 left panel. Cultures were left untreated (solid dots) or exposed to Ag NPs (1.3 μg/mL; triangles) from 2 to 24 h. Upper panels: Expression of *IL1B* and *IL1RN* genes. Lower panels: Rate of production/release of the cytokines IL-1β and IL-1Ra. Data are presented as mean ± SD of three replicate values obtained with monocytes from one representative individual donor.

concomitant increase of the inflammatory cytokine and decrease of the anti-inflammatory cytokine suggests enhanced inflammation. However, it should be noted that during the

Table 2. Peak Expression and Production of Inflammation-Related Factors in the Course of the Inflammatory Reaction *in Vitro*

	peak gene expression (mean AU ± SD)				peak protein production rate (mean pg/h/10^6 cells ± SD)			
inflammation-related factors	peak time	control	Au NPs	solvent	peak time	control	Au NPs	solvent
IL-1α	4 h	4412 ± 717	3872 ± 182	4098 ± 289	24 h	31.8 ± 2.6	32.8 ± 3.1	19.9 ± 1.1*
IL-1R1	9 h	41.5 ± 1.4	34.3 ± 5.2	21.1 ± 4.6	n.t.	n.t.	n.t.	n.t.
IL-1R2	4 h	6.2 ± 1.6	7.7 ± 1.7	7.6 ± 1.2	4 h	132 ± 14	105 ± 15	107 ± 23
IL-18	4 h	2.7 ± 0.5	2.6 ± 0.4	2.3 ± 0.4	4 h	5.1 ± 1.8	5.7 ± 1.4	4.8 ± 0.9
IL-18BP	14 h	8.0 ± 2.1	8.3 ± 3.3	10.4 ± 5.9	4 h	129 ± 0.2	127 ± 8.8	120 ± 9.1
IL-36γ	9 h	6561 ± 969	5823 ± 628	5072 ± 830	ND	ND	ND	ND
IL-6	n.t.	n.t.	n.t.	n.t.	9 h	8686 ± 2420	8191 ± 1696	8707 ± 2538
CCL5	n.t.	n.t.	n.t.	n.t.	4 h	113 ± 35	121 ± 22	123 ± 22

[a]Data are presented as mean ± SD of data obtained with monocytes from three to five individuals. Statistical significance: (*) $p < 0.05$ solvent control vs Au NPs. All other comparisons of Au NPs vs controls (medium/solvent): not significant. n.t. not tested; ND not detectable; AU, arbitrary units.

DOI: 10.1021/acsami.6b06278
ACS Appl. Mater. Interfaces XXXX, XXX, XXX–XXX

resolution phase (24 h) the inflammation-promoting effect of Ag NPs disappears, with IL-1β production going down to background and with IL-1Ra production still sustained. This suggests that the inflammation-enhancing effect of Ag NPs is transient and that human monocytes are fully able to resolve an inflammatory reaction despite the presence of Ag NPs. Gene expression data show little difference upon exposure to Ag NPs, suggesting that the major effect could be on the post-transcriptional phases of cytokine production (Figure 5, upper panels). Evaluation of the production of IL-18 and its inhibitor IL-18BP showed little/no variation in the presence of Ag NPs (data not shown). Solvent had little/no effect (data not shown).

3. DISCUSSION

In this study, Au and Ag NPs were investigated for their immunological safety. We focused on innate/inflammatory immune responses because innate immunity/inflammation is the first defensive reaction that is triggered in response to a potentially dangerous event, and innate immune cells are the first that come in contact with foreign materials in every tissue within the human body. Among innate immune cells we have selected monocytes because these are the inflammatory cells that come from blood into tissues during an inflammatory reaction and are those that detect and eliminate any anomalous agent or material they come in contact with. We have therefore planned to evaluate the possible immunotoxic effects of NPs by setting up *in vitro* a realistic scenario of how NPs would come in contact with defensive cells in a tissue. In a preliminary evaluation, we have assessed the direct effect of the NPs on human monocytes and found that, at the concentrations used (1.3−12 μg/mL), they did not cause monocyte death over 72 h (data not shown). This is in agreement with previous observations on the lack of toxicity of Au NPs for several different cell types[37] and of Ag NPs at low concentrations (below 20 μg/mL).[38,39] In nanotoxicology, inflammatory activation is generally considered as part of the NP toxic effects, since inflammation and generation of reactive oxygen species are usually the step preceding apoptosis and necrosis.[40] However, it should be emphasized that innate immune activation/inflammation is not to be mistaken with toxicity, as this is a key phase in immune defense and does not necessarily lead to cell death. In any case, induction of an innate/immune response, even when not leading to cell death, may be detrimental for medically applied NPs, as uptake and elimination by circulating phagocytes (mainly monocytes) and tissue macrophages will abolish the nanomedicine efficacy.[41] Indeed, a recent review has emphasized the fact that a large part of administrated medical NPs is taken up by the MPS.[30] Therefore, an important objective when designing NPs for medical purposes is to know the features of their interaction with cells of the MPS, in particular for decreasing or eliminating their ability to trigger immune recognition and activation. In this view, we have evaluated the capacity of Au and Ag NPs to induce human cell innate/inflammatory activation in a WBA and in a MAT, by measuring the ability of NPs to induce expression and production of inflammation-related cytokines.[42,43] It is evident that NPs have little/no effect, even at the highest concentration tested, in contrast with the powerful effect induced by a suboptimal concentration of LPS (endotoxin). An important issue should be noted, *i.e.*, that we have tested NPs at concentrations at which the contamination of endotoxin was below the activation threshold. This is important because endotoxin is a potent inducer of innate/inflammatory responses.[29] We observed that when deliberately contaminated with endotoxin, Au NPs acquire the capacity of inducing a significant innate/inflammatory reaction in human monocytes, as opposed to endotoxin-free Au NPs that are ineffective.[44] Therefore, it is important to emphasize that, before performing immunosafety assays, we need to know the possible endotoxin contamination level in the NP preparations, in order to avoid mistaking the effects caused by the contaminating endotoxin for NP-induced effects.[29] Furthermore, we need to further consider the possibility that endotoxin contamination may decrease the effectiveness of *in vivo* administered NPs, due to a more rapid recognition of the endotoxin-coated NPs as foreign entities and their consequent elimination.

After having evaluated the direct activation capacity of NPs for human monocytes, additional information is necessary for a complete assessment of the immunosafety of these particles. In fact, even in the absence of direct induction of inflammation, it is possible that the presence of NPs may positively or negatively affect the normal development of an innate defensive reaction, thereby causing inadequate or excessive responses that may be symptomatic of a prepathological derangement. Thus, testing the effects of NPs on the normal development of the innate/inflammatory responses is an important aspect of their immunosafety profile. We have addressed this issue with a human monocyte-based *in vitro* model of a normal innate/inflammatory defense response that recapitulates, in a simplified manner, the different phases of the reaction, from cell recruitment and initiation of the response, to development of inflammation, and its eventual resolution.

Inflammatory monocytes are recruited into an inflamed tissue in response to chemokines (in particular CCL2) and, once in the tissue, they differentiate into polarized macrophages. M1 macrophages are highly inflammatory and cytocidal cells able to produce inflammatory cytokines, ROS, and proteolytic enzymes, all aiming at destroying the microorganisms or other agents that have initiated the reaction. Conversely, M2 polarization occurs in the changing microenvironment after the causative agent has been eliminated. M2 macrophages produce anti-inflammatory factors that dampen the inflammatory response, actively eliminate debris and damaged cells and matrix, and produce matrix components and mitogenic and angiogenic factors to help reconstructing the damaged tissue.[45−47] The *in vitro* model that we have used for assessing the effects of NPs was designed for recapitulating, in a simplified fashion, the course of an inflammatory reaction, starting from monocyte recruitment, to initial M1 activation/differentiation and eventual reprogramming into the M2 anti-inflammatory tissue-repairing functional phenotype. With all the limitations inherent in *in vitro* models, including the lack of cross-talk with other cells and factors, this model is nevertheless more accurate in reproducing the course of a human *in vivo* inflammatory reaction, in that it is based on human primary cells and it recapitulates kinetically some essential elements of the various phases and conditions of the reaction.

The finding that the model indeed describes the induction of an M1 phenotype and the subsequent passage to the M2 deactivated phenotype validates its reliability.[5] In fact, from a meta-database of all available transcriptomic data on human monocytes and macrophages, we have extracted two lists of genes that characterize the M1 and deactivated M2 phenotypes, respectively. Expression of these genes during the different

DOI: 10.1021/acsami.6b06278
ACS Appl. Mater. Interfaces XXXX, XXX, XXX−XXX

phases of the *in vitro* inflammatory reaction in the monocyte-based model indicates that, during the course of the inflammatory reaction *in vitro*, monocytes become polarized macrophages that adopt first an inflammatory M1-like functional phenotype, and later a resolving M2-like phenotype, suggesting that the model reproduces well the kinetics and characteristics of a resolving *in vivo* inflammation.[5] From the proteomics analysis reported here, it is likewise evident that different biological processes are initiated and differentially modulated during the different phases of the reaction. Although a deeper analysis of the proteomics data is needed, the data so far available suggest this is a realistic model to describe the main phases of monocyte-dependent inflammation *in vivo* in humans. This model could therefore allow us to examine the immunomodulatory effects of NPs in a more reliable and realistic fashion. Among the several factors that vary during the course of the inflammatory reaction, we have selected two, which we intended to use as biomarkers in this and future nanoimmunosafety studies, *i.e.*, the inflammatory cytokine IL-1β and its natural inhibitor IL-1Ra.[34]

IL-1β is among the highly inflammatory cytokines produced during the inflammatory effector phase of the response and is also a key cytokine in the induction and amplification of the ensuing adaptive response.[34] IL-1Ra is the specific receptor antagonist that prevents IL-1β binding to its receptor and consequent signaling. IL-1Ra is typically produced by monocytes in response to the same inflammatory stimuli that induce IL-1β and has a role in keeping under control IL-1β effects during inflammation and shutting them off during resolution. It has been shown that the local balance between IL-1β and IL-1Ra in tissues plays an important role in the development of inflammation in many inflammatory and autoimmune diseases.[48] Hence, we have evaluated the gene expression and the cytokine release for both IL-1β and IL-1Ra as markers for assessing the effects of NPs on the course of the inflammatory reaction *in vitro*.

When Au NPs were tested, it is noteworthy that neither expression nor production of the two factors was affected by the presence of NPs, with the inflammatory phase and the following resolution phase developing with identical kinetics as in the control group. To confirm the results obtained with the prototypical inflammatory/anti-inflammatory cytokine pair IL-1β/IL-1Ra, we have also tested the expression and production of several other cytokines and receptors (released from cells) that are also differentially regulated during the course of inflammation. In particular, we have examined other members of the IL-1 family of cytokines and receptors, *i.e.*, the inflammatory/regulatory cytokine IL-1α, the activating and inhibiting IL-1 receptors IL-1R1 and IL-1R2, the metabolic regulatory/inflammatory cytokine IL-18 and its inhibitor IL-18BP, and the inflammatory cytokine IL-36γ. In addition, we also tested the chemokine CCL5 (RANTES) and the typical inflammatory cytokine IL-6. In no instance the presence of Au NPs did change the level of expression or the rate of production of the various factors examined, nor change the kinetics of their expression or production.

Thus, based on these results, we could say that Au NPs appear immunologically safe for humans, as far as innate immunity and inflammation is concerned, as they do not have direct toxic effects on mononuclear phagocytes, do not induce their activation, and do not interfere with the course of a defensive innate/inflammatory reaction. Thus, the inability of Au NPs to trigger an innate reaction places them in a good position for developing nanomedicines that do not induce destructive immune reactions. The issue remains however that of escaping MPS recognition and elimination. Several *in vivo* studies have addressed the biocompatibility and pharmacokinetics of Au NPs, in particular by examining surface modifications that could allow prolonged half-life in the circulation, likely a consequence of masking from MPS elimination.[49,50] Modification of Au NP surface with polyethylene glycol (PEG) or glutathione can change the Au NP *in vivo* distribution (mouse, rat, or rabbit) and increase the blood half-life without inducing toxic effects (including immunotoxicity measured as alteration of the number of white blood cells).[51−54]

In the case of Ag NPs, it is interesting that some variation was measurable. While variations in gene expression were minimal, the production of the IL-1β cytokine showed a small, but clearly measurable increase in the presence of Ag NPs during the inflammatory phases (4−14 h). On the other hand, the reverse was seen for the production of the IL-1 inhibitor IL-1Ra, which was decreased in the presence of NPs, again during the inflammatory phase. Thus, although Ag NPs were unable to induce either cell death or even inflammatory activation in human monocytes at the endotoxin-free concentrations tested (up to 40 μg/mL; data not shown), at a concentration as low as 1.3 μg/mL they seem to be able to enhance the monocyte inflammatory activation by increasing IL-1 release and decreasing IL-1Ra production. However, it is important to note that this effect is obviously transient, being less evident (at least in the case of IL-1Ra) during late inflammation and being totally absent during the resolution phase. Thus, despite the amplification of the response during the inflammatory phase of the monocyte reaction, such effect is transient, and Ag NPs do not impair or alter the capacity of monocyte to resolve the reaction; thus they do not cause persistence of inflammation. This would suggest that, in endotoxin-free conditions, Ag NPs have a limited and transient inflammation-enhancing effect on human monocytes. The fact that they cannot support a persisting inflammatory reaction suggests that Ag NPs are relatively safe in terms of risk of chronic inflammatory pathologies. Likewise, *in vivo* studies have shown some transient toxicity by Ag NPs. A single dose of 10 mg/kg of 10 nm (but not 40 and 100 nm) Ag NPs could induce acute effects in male CD-1 mice, such as splenic hyperemia, midzonal hepatocellular necrosis, and hemorrhage, after 24 h from intravenous administration,[55] whereas a long-term oral or inhalation exposure did not cause hepatotoxicity, immunotoxicity,[56] or genotoxicity.[57] It should be noted that all the reported *in vivo* studies were aimed at evaluating the direct toxic effects of Au and Ag NPs, whereas no studies were designed for assessing the possible interference of NPs with the development of a defensive innate/inflammatory response.

4. CONCLUSION

The interaction of nanoparticles with the human immune system is a key issue when designing smart nanodrugs/nanocarriers. Besides direct toxic effects on immune cells (cytotoxicity), two other scenarios need to be considered when assessing the immunological risk of NPs, *i.e.*, the induction of an immune reaction and interference with defensive immunological functions. In the first case, NPs may be recognized as potentially dangerous, thereby initiating an immune reaction that would most likely lead to particle engulfment and destruction. This scenario would lead to a double problem,

DOI: 10.1021/acsami.6b06278
ACS Appl. Mater. Interfaces XXXX, XXX, XXX−XXX

the destruction of the nanomedicine and possible damage to the human tissues due to the reaction against the NPs (*e.g.*, inflammation, complement activation). In the second scenario, the presence of NPs may alter the normal course of a defensive immune response, either positively or negatively, leading to situations of excessive or inadequate immunity, both of which may have pathological consequences. We have used Au and Ag NPs at endotoxin-free concentrations, to test their effects on innate immune/inflammatory responses in both scenarios, using representative and valid *in vitro* cell models based on human primary monocytes. The study focused on innate immunity, rather than on adaptive responses, in that innate immune reactions are the first that take place when foreign materials enter the body. In these conditions, Au NPs showed no effect: nontoxic, unable to induce an immune reaction, and unable to interfere with an ongoing immune reaction. On the other hand, Ag NPs were nontoxic and unable to directly induce monocyte inflammatory activation, but they had a transient effect of amplification of the inflammatory response. However, Ag NPs did not have any effect on the capacity of human monocytes to resolve inflammation. We may thus consider Ag NPs as possibly able to induce transient variations of the human innate/inflammatory response, but without consequences or risk of chronic inflammation or damage. An accurate control of the presence of endotoxin contamination in the NP preparations has allowed us to examine the *bona fide* NP effects, in the absence of the confounding inflammatory effects due to endotoxin.

In conclusion, based on the results obtained, we would suggest that human primary cell-based kinetic in vitro assays, such as the one described here, could be more reliable tools (in terms of representativeness of human reactions) for evaluating the immunomodulatory capacities of NPs, even in the absence of overt immunotoxicity. Thus, such assays can well-complement the simpler immunotoxicity assays (such as WBA and MAT). This evaluation of subtle changes in immune responses, which such assays allow us to perform, is very important in the accurate immunosafety testing of nanomaterials, in particular those employed in the design of nanomedicines.

5. EXPERIMENTAL SECTION

5.1. Nanoparticle Synthesis and Characterization. The synthesis and characterization of the NPs used in this work were described in detail previously.[58] Au and Ag NPs were synthesized by the fast addition of $HAuCl_4$ and $AgNO_3$ salts into a Milli-Q water boiling 2.2 mM sodium citrate solution yielding stable and narrowly dispersed 10 nm Au NPs and 14 nm Ag NPs. Resulting NPs were characterized by transmission electron microscopy, ζ-potential measurements, dynamic light scattering, and UV−visible spectrophotometry. Details on the synthesis protocols and characterization methods can be found in the Supporting Information.

5.2. Endotoxin Detection by LAL Assay. The endotoxin contamination of Au and Ag NPs was measured with the chromogenic Pyrochrome LAL assay (catalog no. CD 060; Associates of Cape Cod, Inc., East Falmouth, MA, USA), following the manufacturers' instructions. We adopted a recently established protocol for testing endotoxin in interference-free conditions.[58] In brief, evaluation was performed on at least three different concentrations of particles, previously tested for lack of interference with the assay's optical readout, and which had an acceptable value of recovery rate (assessed by running the positive product controls that evaluate the NP interference with the assay components).

5.3. Monocyte Isolation from Peripheral Blood. Human peripheral blood mononuclear cells (PBMC) were separated from buffy coats of healthy donors (see the section Ethics Statement) by gradient density centrifugation on Ficoll-Paque PLUS (GE Healthcare, Bio-Sciences AB, Uppsala, Sweden). Monocytes were isolated from PBMC using the Monocyte Isolation kit II (Miltenyi Biotec, Bergisch-Gladbach, Germany) according to the manufacturer's protocol. The purity of the isolated monocytes (>98%) was determined by differential counts on cytocentrifuge smears stained with a modified Wright-Giemsa dye (Diff Quik, Medion Diagnostics AG, Düdingen, Switzerland). Viability was determined by trypan blue dye exclusion and always exceeded 98%.

5.4. Nanoparticle Dispersion in Culture Medium for *in Vitro* Experiments. NPs were preincubated with heat-inactivated human AB serum (Sigma-Aldrich, Inc., St. Louis, MO, USA) for 1 h at 37 °C before addition to monocytes in culture. Briefly, 1 mL of NP stock solution was centrifuged to remove the solvent, and the NPs were resuspended in 1 mL of human AB serum and incubated for 1 h at 37 °C. Then, the NP suspension in serum was added to culture medium so as to reach the final NP concentrations 1.3, 4, and 12 μg/mL and the final serum concentration (5%).

For deliberate contamination of Au NPs with endotoxin, 1 mL of Au NPs was incubated with 1 μg/mL *Escherichia coli* (*E. coli*) LPS (from *E. coli* serotype 055:B5; catalog no. L6529, Sigma-Aldrich) for 1 h at room temperature (RT), then collected by ultracentrifugation at 36000*g* for 40 min. Two washing steps were performed with endotoxin-free water to eliminate the unbound LPS. The endotoxin-contaminated Au NPs were finally resuspended in human AB serum and incubated for 1 h at 37 °C, as described above, before addition to the cell cultures.

No evidence of NP aggregation was found after these procedures.

5.5. Monocyte Activation Test. Monocytes were cultured at a density of 2.5×10^6 cells/well in 12-well culture plates (Corning Inc., Costar, New York, NY, USA) in 1 mL of RPMI 1640+glutamax-I medium (GIBCO by Life Technologies, Paisley, U.K.) supplemented with 50 μg/mL Gentamicin (GIBCO) and 5% heat-inactivated human AB serum at 37 °C in moist air with 5% CO_2. Monocytes were exposed to NPs for 24 h. Supernatant and cells were collected for further analysis.

5.6. Whole Blood Assay. Human blood was withdrawn from healthy donors. Heparinized blood samples were diluted 1:4 (v/v) with culture medium alone, or medium plus LPS (2.5 ng/mL), or medium plus Au or Ag NPs at different concentrations, in a final volume of 1 mL. After 24 h of incubation at 37 °C, 100 μL of 5% Triton-X were added to each tube for lysing the cells; tubes were immediately frozen to complete the lysis and kept at −80 °C until use. The blood lysates were centrifuged at 3000*g* for 10 min before cytokine measurement by ELISA.

5.7. *In Vitro* Kinetic Model of a Resolving Inflammatory Response. The model adopted in this study is based on that described in a previous publication,[5] with slight modifications for improving performance (shorter time, lower costs). Based on comparative analysis, the modified model maintains the same characteristics as those of the published model (data not shown and Figure 4). Monocytes were cultured at a density of 2.5×10^6 cells/well in 12-well culture plates and sequentially exposed to different temperatures and cytokines during 24 h of culture, to mimic the microenvironmental conditions of an inflamed tissue. All human recombinant cytokines were obtained from R&D Systems (Minneapolis, MN, USA). Concentrations used were as follows: CCL2, 20 ng/mL; LPS, 5 ng/mL; TNF-α, 10 ng/mL; IFN-γ, 25 ng/mL.

The *in vitro* stimulation was performed as described in Results and summarized in Figure 3. NPs were preincubated with human AB serum for 1 h at 37 °C and added to monocytes from 2 to 24 h. Exposure to DXM (Sigma-Aldrich) and CL097 (InvivoGen, San Diego, CA, USA) was performed from 2 to 14 h. Medium throughout the experiment was RPMI 1640+glutamax-I medium +50 μg/mL Gentamicin and 5% heat-inactivated human AB serum.

Freshly isolated monocytes were taken as time 0. For RNA isolation, cells were harvested in 700 μL of Qiazol (Qiagen, Hilden, Germany) at times 0, 4, 9, 14, and 24 h. Supernatants were collected at times 2, 4, 9, 14, and 24 h. All samples were stored at −80 °C until use.

DOI: 10.1021/acsami.6b06278
ACS Appl. Mater. Interfaces XXXX, XXX, XXX−XXX

5.8. Monocyte Viability. Viability of monocytes in culture was determined both in the MAT and in the kinetic model by trypan blue dye exclusion at the end of the culture. During culture, viability was assessed visually by phase contrast microscopy. In no case cell viability in NP-treated cultures differed from that in control and solvent-treated cultures (data not shown).

5.9. RNA Extraction and Quantitative PCR Analysis. RNA extractions were performed using Qiagen miRNeasy kit (Qiagen), according to the manufacturer's protocol. RNA samples were quantified by ND-1000 spectrophotometer (NanoDrop Technologies, Wilmington, DE, USA), and RNA integrity was checked by microcapillary electrophoresis on Agilent 2100 Bioanalyzer (Agilent Technologies, Palo Alto, CA, USA) on the basis of the ratio between 28S and 18S rRNA peak areas and of the RIN (RNA integrity number) index (≥8). RNA samples were stored at −80 °C until use.

cDNAs were reverse transcribed from total RNA (300 ng per sample) according to the QuantiTect Reverse Transcription Kit (Qiagen) instructions, with oligo-dT and random primers, to allow for high cDNA yield. Three separate reverse transcriptions were performed for each sample, and an identical reaction without reverse transcriptase was run as negative control. Taqman quantitative polymerase chain reaction (PCR) was performed with a Rotor-Gene 3000 (Corbett Research, Doncaster, Victoria, Australia), using the QuantiTect SYBR Green PCR Master Mix (Qiagen). The final reaction contained 12.5 μL of 2× QuantiTect SYBR Green PCR Master Mix, 0.3 μM of each primer, and 2.5 μL of cDNA in a total volume of 25 μL. PCR conditions were 94 °C for 15 min, followed by 35−40 cycles of 94 °C for 15 s, 50−60 °C for 30 s, and 72 °C for 30 s. Primer sequences were supplied by Qiagen both for target genes (*IL1A*, *IL1B*, *IL1RN*, *IL1R1*, *IL1R2*, *IL36G*, *IL18*, and *IL18BP*) and housekeeping genes (*ACTB* and *GAPDH*). Relative gene expressions were calculated using the efficiency correction method, which calculates the relative expression ratio of a target gene based on the qPCR efficiencies and the Ct of samples vs controls (fresh monocytes at time 0 in the kinetic experiments, or medium-treated controls in the MAT), expressed in comparison to the calibrator housekeeping genes.[59]

5.10. Protein Detection by ELISA. IL-1α, IL-1β, IL-1Ra, sIL-1R2, IL-18, IL-18BP, IL-6, and CCL5 were measured in the supernatants collected at different times (2, 4, 9, 14, and 24 h) by enzyme-linked immunosorbent assay (ELISA). All ELISA kits were purchased from R&D Systems, except for the IL-18 kit that was obtained from MBL (Nagoya Aichi, Japan), and for the IL-36γ kits, provided by USCNK Life Science Inc. (Wuhan, China) and Innovative Research, Inc. (Novi, MI, USA). ELISA assays were performed according to the manufacturers' instructions. Each sample was assayed in duplicate, and detection performed with a microplate spectrophotometer (JUPITER; Asys Hitech GmbH, Eugendorf, Austria). Data are expressed as picograms of produced cytokines per million input cells unless otherwise stated.

5.11. Proteomics Analysis. Monocytes were isolated from three different individuals and cultured at a density of 5×10^6 cells/well in 6-well culture plates (Costar, Corning). Monocytes were kinetically stimulated *in vitro* as described above (section In Vitro Kinetic Model of a Resolving Inflammatory Response). Cells were collected in 200 μL of RIPA buffer (catalog no. 89900, Thermo Fisher Scientific, Inc., Waltham, MA, USA) containing 2 μL of protease inhibitor (catalog no. 78425, Thermo Fisher Scientific) and 2 μL of phosphatase inhibitor (catalog no. 78420, Thermo Fisher Scientific), and then kept at −80 °C until use.

5.11.1. Protein Extraction. Cells were lysed by sonication (2× for 30 s). After shaking on ice for 15 min, cells were centrifuged for 15 min at 14000*g* to remove debris. Protein concentration was determined by the Pierce BCA protein assay kit (catalog no. 23225, Thermo Fisher Scientific). Then, 20 μg of each sample was mixed−linked with 0.1% RapiGest SF Surfactant (catalog no. 186001860, Waters, Milford, MA, USA). Samples were incubated for 5 min at 100 °C and then placed on ice immediately.

5.11.2. Acetone Precipitation and Trypsin Digestion. The following mixtures were used: 200 mM TCEP kit (70 μL of 0.5 M Tris (2-carboxyethyl)phosphine hydrochloride (TCEP, Thermo Fisher Scientific) + 70 μL of H_2O + 35 μL of 1 M tetraethylammonium bromide (TEAB T7408, Sigma-Aldrich)) and 375 mM IAA mixture (9 mg of indole-3-acetic acid (IAA) dissolved in 132 μL of 200 mM TEAB). A 1 μL aliquot of the 200 mM TCEP mixture was added to the samples (20 μg of protein) and incubated for 1 h at 55 °C. Then, 1 μL of the 375 mM IAA mixture was added to each sample, followed by 30 min incubation at RT in the dark. Six volumes of cold acetone (−20 °C) were added to the samples and incubated overnight at −20 °C. Then, the samples were centrifuged for 10 min at 10000*g* at 4 °C, and the supernatants were removed without drying the samples. The pellet was dissolved in 20 μL of 100 mM TEAB and 1 μg of trypsin was added at a 1:20 ratio. Then, the samples were incubated overnight at 37 °C. Next, HCl was added to the samples to a final concentration of 200 mM, followed by incubation for 30 min and centrifugation for 10 min at 10000*g*. Pellets were removed after the centrifugation step.

5.11.3. Labeling and Desalting. Each 10 μg sample was added to one aliquot of tandem mass tag (TMT)-label (TMT Mass Tagging Kits and Reagents; catalog no. 90064, Thermo Fisher Scientific). After vortexing and spinning, the samples were incubated for 1 h at RT. A 4 μL aliquot of 5 mM hydroxylamine (diluted 1:10 in 200 mM TEAB) was added to the samples, which were incubated for 15 min at RT. Finally, five differently labeled samples (five different time points) from one experiment of one individual (control or NPs) were combined. The combined samples were desalted using C18 Pierce spin columns (Thermo Fisher Scientific) with 20% acetonitrile (ACN) washing.

After desalting, the samples (100 μg each) were further fractionated using an ACQUIT UPLC System (Waters) with an XBridge BEH130 C18 column at 40 °C (mobile phases (MP), 400 μL; MFA, 2% ACN; MFB, 98% ACN; pH = 9). Samples were dissolved in 30 μL of 5% ACN, and 10 fractions were taken for each sample. Then, the LC-MS/MS analysis was performed on these samples using the LTQ-velos Orbitrap hybrid mass spectrometry platform (Thermo Fisher Scientific).

5.11.4. Proteomics Data Analysis. Proteome discoverer (1.3) software (Thermo Fisher Scientific) was used to perform database searching against the IPI Human 3.87 database using both Sequest and Mascot algorithms on each of the six TMT LC-MS runs. The results were filtered using the following settings: only medium and high confident peptides with a global FDR < 5% and first ranked peptides were included in the results. In the TMT quantitation workflow, the most confident centroid method was used with an integration window of 20 ppm. The reporter ion intensities were justified for isotope contamination by solving a system of linear equations and the known label purity values from the TMT data sheet. Consecutively, reporter ion intensities were corrected for systematic effects that originate from sample preparation and labeling with the CONSTANd normalization. All the sequences and reporter ion intensities of the unique peptides that match previous requirements were exported to comma-separated values for further data analysis using in-house scripts. Normalized reporter ion intensities were presented to a hierarchical clustering algorithm with Spearman rank correlation as a distance measure and unweighted average distance linkage.[60−62] Clustering was performed on the peptides dimension that resulted in a dendrogram, displayed at the left-hand site of the heat-map diagram.

5.12. Statistical Analysis. Data are presented as mean ± SD of values from replicate cultures of one representative experiment of at least three independent experiments performed (when the inter-individual quantitative variability was too high for allowing averaging), or mean ± SD of values from more than three individual donors (the exact number of donors is indicated in the legend of each figure). Statistical significance was calculated by Student's *t*-test. A p value < 0.05 was considered as statistically significant.

5.13. Ethics Statement. There is no ethical approval or informed consent required by the Italian law for discarded blood products. The use of the blood samples from normal donors for the study of monocyte activation and polarization was included in a collaborative research with Prof. Paola Migliorini, which was approved by the Ethical Committee of the University of Pisa S. Chiara Hospital (prot.

DOI: 10.1021/acsami.6b06278
ACS Appl. Mater. Interfaces XXXX, XXX, XXX−XXX

AOUP 33998 of Sep. 29, 2006), and which is still ongoing. All samples of human blood included in this study were from anonymous donors and were donated by Prof. Migliorini.

■ ASSOCIATED CONTENT

Supporting Information

The Supporting Information is available free of charge on the ACS Publications website at DOI: 10.1021/acsami.6b06278.

Experimental details of the synthesis and characterization of NPs, (Figure S1) IL-6 production in human monocytes *in vitro*, (Figure S2) IL-1 family gene expression in primary human monocytes exposed to Au nanoparticles, (Figure S3) Endotoxin-contaminated Au nanoparticles induce inflammatory activation of monocytes, (Figure S4) modulation of IL-1β release in monocytes by immunostimulatory and immunosuppressive agents *in vitro*, (Figure S5) molecular function, cellular component, and biological process ontologies for the yellow, blue, and red peptide clusters, and (Figure S6) dose−response analysis of the effect of Au nanoparticles on the course of the inflammatory reaction *in vitro* (PDF)

■ AUTHOR INFORMATION

Corresponding Author

*E-mail: yang.li.nano@gmail.com; yang.3.li@ucdenver.edu.

Present Address

[○]Department of Dermatology, University of Colorado Anschutz Medical Campus, Aurora, CO 80045, USA.

Notes

The authors declare no competing financial interest.

■ ACKNOWLEDGMENTS

We are grateful to Maria Domenica Costantino (ITB, CNR, Pisa, Italy) and Linda C. Stöhr (Grimm Aerosol, Ainring, Germany) for their contribution to the *in vitro* experiments and to Prof. Albert Duschl (University of Salzburg, Austria) for helpful discussion. We also thank Prof. Paola Migliorini from the University of Pisa S. Chiara Hospital (Italy) for providing all the human blood samples used in this study. This study was supported by the EU FP7 projects NanoTOES (PITN-GA-2010-264506), QualityNano (INFRA-2010-262163; TA Project, VITO-TAF-223) and NANoREG (NMP4-LA2013-3105984) and by the H2020 project PANDORA (MSCA-ITN-2015-671881).

■ REFERENCES

(1) Murphy, K. M.; *Janeway's Immunobiology*, 8th ed; Garland Science: New York, 2012.

(2) Wynn, T. A.; Chawla, A.; Pollard, J. W. Macrophage Biology in Development, Homeostasis and Disease. *Nature* **2013**, *496*, 445−455.

(3) Li, Y.; Liu, Y.; Fu, Y.; Wei, T.; Le Guyader, L.; Gao, G.; Liu, R. S.; Chang, Y. Z.; Chen, C. The Triggering of Apoptosis in Macrophages by Pristine Graphene through the MAPK and TGF-beta Signaling Pathways. *Biomaterials* **2012**, *33*, 402−411.

(4) Boraschi, D.; Costantino, L.; Italiani, P. Interaction of Nanoparticles with Immunocompetent Cells: Nanosafety Considerations. *Nanomedicine* **2012**, *7*, 121−131.

(5) Italiani, P.; Mazza, E. M.; Lucchesi, D.; Cifola, I.; Gemelli, C.; Grande, A.; Battaglia, C.; Bicciato, S.; Boraschi, D. Transcriptomic Profiling of the Development of the Inflammatory Response in Human Monocytes In Vitro. *PLoS One* **2014**, *9*, e87680.

(6) Sperling, R. A.; Rivera Gil, P.; Zhang, F.; Zanella, M.; Parak, W. J. Biological Applications of Gold Nanoparticles. *Chem. Soc. Rev.* **2008**, *37*, 1896−1908.

(7) El-Sayed, I. H.; Huang, X.; El-Sayed, M. A. Surface Plasmon Resonance Scattering and Absorption of Anti-EGFR Antibody Conjugated Gold Nanoparticles in Cancer Diagnostics: Applications in Oral Cancer. *Nano Lett.* **2005**, *5*, 829−834.

(8) Cheheltani, R.; Ezzibdeh, R. M.; Chhour, P.; Pulaparthi, K.; Kim, J.; Jurcova, M.; Hsu, J. C.; Blundell, C.; Litt, H. I.; Ferrari, V. A.; Allcock, H. R.; Sehgal, C. M.; Cormode, D. P. Tunable, Biodegradable Gold Nanoparticles as Contrast Agents for Computed Tomography and Photoacoustic Imaging. *Biomaterials* **2016**, *102*, 87−97.

(9) Wang, H.; Huff, T. B.; Zweifel, D. A.; He, W.; Low, P. S.; Wei, A.; Cheng, J.-X. In Vitro and in Vivo Two-Photon Luminescence Imaging of Single Gold Nanorods. *Proc. Natl. Acad. Sci. U. S. A.* **2005**, *102*, 15752−15756.

(10) Xu, L.; Liu, Y.; Chen, Z.; Li, W.; Liu, Y.; Wang, L.; Liu, Y.; Wu, X.; Ji, Y.; Zhao, Y.; Ma, L.; Shao, Y.; Chen, C. Surface-Engineered Gold Nanorods: Promising DNA Vaccine Adjuvant for HIV-1 Treatment. *Nano Lett.* **2012**, *12*, 2003−2012.

(11) Ghosh, P.; Han, G.; De, M.; Kim, C. K.; Rotello, V. M. Gold Nanoparticles in Delivery Applications. *Adv. Drug Delivery Rev.* **2008**, *60*, 1307−1315.

(12) Zhang, Z.; Wang, L.; Wang, J.; Jiang, X.; Li, X.; Hu, Z.; Ji, Y.; Wu, X.; Chen, C. Mesoporous Silica-Coated Gold Nanorods as a Light-Mediated Multifunctional Theranostic Platform for Cancer Treatment. *Adv. Mater.* **2012**, *24*, 1418−1423.

(13) Sonavane, G.; Tomoda, K.; Makino, K. Biodistribution of Colloidal Gold Nanoparticles after Intravenous Administration: Effect of Particle Size. *Colloids Surf., B* **2008**, *66*, 274−280.

(14) Cho, E. C.; Zhang, Q.; Xia, Y. The Effect of Sedimentation and Diffusion on Cellular Uptake of Gold Nanoparticles. *Nat. Nanotechnol.* **2011**, *6*, 385−391.

(15) Qiu, Y.; Liu, Y.; Wang, L.; Xu, L.; Bai, R.; Ji, Y.; Wu, X.; Zhao, Y.; Li, Y.; Chen, C. Surface Chemistry and Aspect Ratio Mediated Cellular Uptake of Au Nanorods. *Biomaterials* **2010**, *31*, 7606−7619.

(16) Yen, H. J.; Hsu, S. h.; Tsai, C. L. Cytotoxicity and Immunological Response of Gold and Silver Nanoparticles of Different Sizes. *Small* **2009**, *5*, 1553−1561.

(17) Ashraf, S.; Pelaz, B.; del Pino, P.; Carril, M.; Escudero, A.; Parak, W. J.; Soliman, M. G.; Zhang, Q.; Carrillo-Carrion, C. Gold-Based Nanomaterials for Applications in Nanomedicine. In *Light-Responsive Nanostructured Systems for Applications in Nanomedicine*; Springer: Cham, Switzerland, 2016; pp 169−202, DOI: 10.1007/978-3-319-22942-3_6.

(18) Zhang, D.; Neumann, O.; Wang, H.; Yuwono, V. M.; Barhoumi, A.; Perham, M.; Hartgerink, J. D.; Wittung-Stafshede, P.; Halas, N. J. Gold Nanoparticles Can Induce the Formation of Protein-Based Aggregates at Physiological pH. *Nano Lett.* **2009**, *9*, 666−671.

(19) Alkilany, A. M.; Murphy, C. J. Toxicity and Cellular Uptake of Gold Nanoparticles: What We Have Learned So Far? *J. Nanopart. Res.* **2010**, *12*, 2313−2333.

(20) Abou El-Nour, K. M. M.; Eftaiha, A.; Al-Warthan, A.; Ammar, R. A. A. Synthesis and Applications of Silver Nanoparticles. *Arabian J. Chem.* **2010**, *3*, 135−140.

(21) Rai, M.; Yadav, A.; Gade, A. Silver Nanoparticles as a New Generation of Antimicrobials. *Biotechnol. Adv.* **2009**, *27*, 76−83.

(22) Kim, J. S.; Kuk, E.; Yu, K. N.; Kim, J.-H.; Park, S. J.; Lee, H. J.; Kim, S. H.; Park, Y. K.; Park, Y. H.; Hwang, C.-Y.; Kim, Y.-K.; Lee, Y.-S.; Jeong, D. H.; Cho, M.-H. Antimicrobial Effects of Silver Nanoparticles. *Nanomedicine (N. Y., NY, U. S.)* **2007**, *3*, 95−101.

(23) AshaRani, P.; Low Kah Mun, G.; Hande, M. P.; Valiyaveettil, S. Cytotoxicity and Genotoxicity of Silver Nanoparticles in Human Cells. *ACS Nano* **2009**, *3*, 279−290.

(24) Greulich, C.; Kittler, S.; Epple, M.; Muhr, G.; Köller, M. Studies on the Biocompatibility and the Interaction of Silver Nanoparticles with Human Mesenchymal Stem Cells (hMSCs). *Langenbeck. Arch. Surg.* **2009**, *394*, 495−502.

DOI: 10.1021/acsami.6b06278
ACS Appl. Mater. Interfaces XXXX, XXX, XXX−XXX

(25) Kittler, S.; Greulich, C.; Diendorf, J.; Koller, M.; Epple, M. Toxicity of Silver Nanoparticles Increases During Storage Because of Slow Dissolution under Release of Silver Ions. *Chem. Mater.* **2010**, *22*, 4548−4554.
(26) Kim, S.; Choi, J. E.; Choi, J.; Chung, K.-H.; Park, K.; Yi, J.; Ryu, D.-Y. Oxidative Stress-Dependent Toxicity of Silver Nanoparticles in Human Hepatoma Cells. *Toxicol. In Vitro* **2009**, *23*, 1076−1084.
(27) Park, E.-J.; Yi, J.; Kim, Y.; Choi, K.; Park, K. Silver Nanoparticles Induce Cytotoxicity by a Trojan-Horse Type Mechanism. *Toxicol. In Vitro* **2010**, *24*, 872−878.
(28) Izak-Nau, E.; Huk, A.; Reidy, B.; Uggerud, H.; Vadset, M.; Eiden, S.; Voetz, M.; Himly, M.; Duschl, A.; Dusinska, M.; Lynch, I. Impact of Storage Conditions and Storage Time on Silver Nanoparticles' Physicochemical Properties and Implications for Their Biological Effects. *RSC Adv.* **2015**, *5*, 84172−84185.
(29) Li, Y.; Boraschi, D. Endotoxin Contamination: A Key Element in the Interpretation of Nanosafety Studies. *Nanomedicine* **2016**, *11*, 269−287.
(30) Wilhelm, S.; Tavares, A. J.; Dai, Q.; Ohta, S.; Audet, J.; Dvorak, H. F.; Chan, W. C. Analysis of Nanoparticle Delivery to Tumours. *Nat. Rev. Mater.* **2016**, *1*, 16014.
(31) Schlinkert, P.; Casals, E.; Boyles, M.; Tischler, U.; Hornig, E.; Tran, N.; Zhao, J.; Himly, M.; Riediker, M.; Oostingh, G. J.; Puntes, V.; Duschl, A. The Oxidative Potential of Differently Charged Silver and Gold Nanoparticles on Three Human Lung Epithelial Cell Types. *J. Nanobiotechnol.* **2015**, *13*, 1.
(32) Casals, E.; Pfaller, T.; Duschl, A.; Oostingh, G. J.; Puntes, V. F. Hardening of the Nanoparticle-Protein Corona in Metal (Au, Ag) and Oxide (Fe_3O_4, CoO, and CeO_2) Nanoparticles. *Small* **2011**, *7*, 3479−3486.
(33) Casals, E.; Pfaller, T.; Duschl, A.; Oostingh, G. J.; Puntes, V. Time Evolution of the Nanoparticle Protein Corona. *ACS Nano* **2010**, *4*, 3623−3632.
(34) Dinarello, C. A. Immunological and Inflammatory Functions of the Interleukin-1 Family. *Annu. Rev. Immunol.* **2009**, *27*, 519−550.
(35) Supek, F.; Bošnjak, M.; Škunca, N.; Šmuc, T. Revigo Summarizes and Visualizes Long Lists of Gene Ontology Terms. *PLoS One* **2011**, *6*, e21800.
(36) Oostingh, G. J.; Casals, E.; Italiani, P.; Colognato, R.; Stritzinger, R.; Ponti, J.; Pfaller, T.; Kohl, Y.; Ooms, D.; Favilli, F.; et al. Problems and Challenges in the Development and Validation of Human Cell-Based Assays to Determine Nanoparticle-Induced Immunomodulatory Effects. *Part. Fibre Toxicol.* **2011**, *8*, 8.
(37) Pfaller, T.; Puntes, V.; Casals, E.; Duschl, A.; Oostingh, G. J. In Vitro Investigation of Immunomodulatory Effects Caused by Engineered Inorganic Nanoparticles-the Impact of Experimental Design and Cell Choice. *Nanotoxicology* **2009**, *3*, 46−59.
(38) Gliga, A. R.; Skoglund, S.; Odnevall Wallinder, I.; Fadeel, B.; Karlsson, H. L. Size-Dependent Cytotoxicity of Silver Nanoparticles in Human Lung Cells: The Role of Cellular Uptake, Agglomeration and Ag Release. *Part. Fibre Toxicol.* **2014**, *11*, 11.
(39) Singh, R. P.; Ramarao, P. Cellular Uptake, Intracellular Trafficking and Cytotoxicity of Silver Nanoparticles. *Toxicol. Lett.* **2012**, *213*, 249−259.
(40) Nel, A.; Xia, T.; Mädler, L.; Li, N. Toxic Potential of Materials at the Nanolevel. *Science* **2006**, *311*, 622−627.
(41) Shah, N. B.; Vercellotti, G. M.; White, J. G.; Fegan, A.; Wagner, C. R.; Bischof, J. C. Blood−Nanoparticle Interactions and in Vivo Biodistribution: Impact of Surface PEG and Ligand Properties. *Mol. Pharmaceutics* **2012**, *9*, 2146−2155.
(42) FDA; CDER; CBER; CMV; CDRH; ORA. *Guidance for Industry. Pyrogen and Endotoxins Testing: Questions and Answers*; U.S. Food and Drug Administration: Silver Spring, MD, USA, 2012.
(43) Kikkert, R.; De Groot, E. R.; Aarden, L. A. Cytokine Induction by Pyrogens: Comparison of Whole Blood, Mononuclear Cells, and TLR-Transfectants. *J. Immunol. Methods* **2008**, *336*, 45−55.
(44) Li, Y.; Tran, N.; Puntes, V. F.; Boraschi, D. Bacterial Endotoxin Binds to the Surface of Gold Nanoparticles and Triggers Inflammation. *7th International Nanotoxicology Congress—NanoTox 2014*, Antalya, Turkey, Apr. 23−26, 2014; International Nanotoxicology Congress,2014; p 142.
(45) Mills, C. D.; Kincaid, K.; Alt, J. M.; Heilman, M. J.; Hill, A. M. M-1/M-2 Macrophages and the Th1/Th2 Paradigm. *J. Immunol.* **2000**, *164*, 6166−6173.
(46) Martinez, F. O.; Sica, A.; Mantovani, A.; Locati, M. Macrophage Activation and Polarization. *Front. Biosci., Landmark Ed.* **2008**, *13*, 453−461.
(47) Italiani, P.; Boraschi, D. From Monocytes to M1/M2 Macrophages: Phenotypical vs. Functional Differentiation. *Front. Immunol.* **2014**, *5*, 514.
(48) Palomo, J.; Dietrich, D.; Martin, P.; Palmer, G.; Gabay, C. The Interleukin (IL)-1 Cytokine Family-Balance between Agonists and Antagonists in Inflammatory Diseases. *Cytokine* **2015**, *76*, 25−37.
(49) Johnston, H. J.; Hutchison, G.; Christensen, F. M.; Peters, S.; Hankin, S.; Stone, V. A Review of the in Vivo and in Vitro Toxicity of Silver and Gold Particulates: Particle Attributes and Biological Mechanisms Responsible for the Observed Toxicity. *Crit. Rev. Toxicol.* **2010**, *40*, 328−346.
(50) Khlebtsov, N.; Dykman, L. Biodistribution and Toxicity of Engineered Gold Nanoparticles: A Review of in Vitro and in Vivo Studies. *Chem. Soc. Rev.* **2011**, *40*, 1647−1671.
(51) Simpson, C. A.; Huffman, B. J.; Gerdon, A. E.; Cliffel, D. E. Unexpected Toxicity of Monolayer Protected Gold Clusters Eliminated by PEG-Thiol Place Exchange Reactions. *Chem. Res. Toxicol.* **2010**, *23*, 1608−1616.
(52) Simpson, C. A.; Salleng, K. J.; Cliffel, D. E.; Feldheim, D. L. In Vivo Toxicity, Biodistribution, and Clearance of Glutathione-Coated Gold Nanoparticles. *Nanomedicine (N. Y., NY, U. S.)* **2013**, *9*, 257−263.
(53) Glazer, E. S.; Zhu, C.; Hamir, A. N.; Borne, A.; Thompson, C. S.; Curley, S. A. Biodistribution and Acute Toxicity of Naked Gold Nanoparticles in a Rabbit Hepatic Tumor Model. *Nanotoxicology* **2011**, *5*, 459−468.
(54) Lipka, J.; Semmler-Behnke, M.; Sperling, R. A.; Wenk, A.; Takenaka, S.; Schleh, C.; Kissel, T.; Parak, W. J.; Kreyling, W. G. Biodistribution of PEG-Modified Gold Nanoparticles Following Intratracheal Instillation and Intravenous Injection. *Biomaterials* **2010**, *31*, 6574−6581.
(55) Recordati, C.; De Maglie, M.; Bianchessi, S.; Argentiere, S.; Cella, C.; Mattiello, S.; Cubadda, F.; Aureli, F.; D'Amato, M.; Raggi, A.; Lenardi, C.; Milani, P.; Scanziani, E. Tissue Distribution and Acute Toxicity of Silver after Single Intravenous Administration in Mice: Nano-Specific and Size-Dependent Effects. *Part. Fibre Toxicol.* **2015**, *13*, 12.
(56) van der Zande, M.; Vandebriel, R. J.; Van Doren, E.; Kramer, E.; Herrera Rivera, Z.; Serrano-Rojero, C. S.; Gremmer, E. R.; Mast, J.; Peters, R. J.; Hollman, P. C.; Hendriksen, P. J. M.; Marvin, H. J. P.; Peijnenburg, A. A. C. M.; Bouwmeester, H. Distribution, Elimination, and Toxicity of Silver Nanoparticles and Silver Ions in Rats after 28-Day Oral Exposure. *ACS Nano* **2012**, *6*, 7427−7442.
(57) Kim, J. S.; Sung, J. H.; Ji, J. H.; Song, K. S.; Lee, J. H.; Kang, C. S.; Yu, I. J. In Vivo Genotoxicity of Silver Nanoparticles after 90-Day Silver Nanoparticle Inhalation Exposure. *SH W* **2011**, *2*, 34−38.
(58) Li, Y.; Italiani, P.; Casals, E.; Tran, N.; Puntes, V. F.; Boraschi, D. Optimising the Use of Commercial Lal Assays for the Analysis of Endotoxin Contamination in Metal Colloids and Metal Oxide Nanoparticles. *Nanotoxicology* **2015**, *9*, 462−473.
(59) Pfaffl, M. W. A New Mathematical Model for Relative Quantification in Real-Time RT-PCR. *Nucleic Acids Res.* **2001**, *29*, e45.
(60) Bar-Joseph, Z.; Gifford, D. K.; Jaakkola, T. S. Fast Optimal Leaf Ordering for Hierarchical Clustering. *Bioinformatics* **2001**, *17*, S22−S29.
(61) DeRisi, J. L.; Iyer, V. R.; Brown, P. O. Exploring the Metabolic and Genetic Control of Gene Expression on a Genomic Scale. *Science* **1997**, *278*, 680−686.
(62) Faust, K.; Croes, D.; van Helden, J. Prediction of Metabolic Pathways from Genome-Scale Metabolic Networks. *BioSystems* **2011**, *105*, 109−121.

DOI: 10.1021/acsami.6b06278
ACS Appl. Mater. Interfaces XXXX, XXX, XXX−XXX